

CrossMark  
click for updates

# Nature of conductivity in SrSiO<sub>3</sub>-based fast ion conductors†

C. Tealdi,\* L. Malavasi, I. Uda, C. Ferrara, V. Berbenni and P. Mustarelli

Cite this: *Chem. Commun.*, 2014, 50, 14732Received 5th September 2014,  
Accepted 30th September 2014

DOI: 10.1039/c4cc07025a

www.rsc.org/chemcomm

**In this paper we report the preparation and characterization of Sr<sub>1-x</sub>Na<sub>x</sub>SiO<sub>3-0.5x</sub> samples, recently proposed as oxide ion conductors. We show that Na-doping unlikely takes place in the silicate phase, and that a secondary glassy phase is at the origin of the transport properties, thereby suggesting that the conductivity is due only to a limited extent to oxide ion migration in the crystalline system.**

Research efforts devoted to the improvement of material properties in the field of solid oxide fuel cells (SOFCs) are extremely active: new compositions as well as ways of improving the performances of existing materials are constantly explored.<sup>1</sup> One of the major challenges in this area is lowering the operating temperature to the intermediate temperature regime (<700 °C) while maintaining good electrochemical performances. In this picture, the solid electrolyte plays a central role since its ionic conductivity determines the best operating temperature range. Novel compounds include oxygen-deficient materials possessing the perovskite crystal structure,<sup>2</sup> and interstitial-oxygen materials belonging to the families of apatite, melilite<sup>1</sup> and scheelite<sup>3</sup> crystal structures.

Recently, the Sr<sub>1-x</sub>K<sub>x</sub>MO<sub>3-0.5x</sub> (with M = Si, Ge) family was proposed as a highly promising novel class of electrolyte materials showing good conductivity values ( $\sigma \geq 10^{-2}$  S cm<sup>-1</sup>) at intermediate temperatures.<sup>4</sup> K-doped samples in this system were subsequently shown to be highly hygroscopic at room temperature, while Na-doping was proved to be highly effective in introducing purely oxide ion conduction in the system, thanks also to the large range of solubility of Na ions on the Sr site.<sup>5,6</sup> Such a solubility, extending up to the composition Sr<sub>0.55</sub>Na<sub>0.45</sub>SiO<sub>2.775</sub>, gives origin to a remarkable oxide ion conductivity ( $\sigma \geq 10^{-2}$  S cm<sup>-1</sup> at  $T < 500$  °C) and is associated with a very low activation energy for oxide ion migration of about 0.3 eV; the stability range of the ionic conductivity as a function of the oxygen partial pressure was

shown to extend down to 10<sup>-30</sup> atm.<sup>6</sup> Based on such values, the Sr<sub>0.55</sub>Na<sub>0.45</sub>SiO<sub>2.775</sub> composition represents the best performing electrolyte material for SOFC currently known for temperatures lower than 650 °C.<sup>6</sup>

The parent SrSiO<sub>3</sub> compound is constituted by layers of Sr<sup>2+</sup> ions spaced by Si<sub>3</sub>O<sub>9</sub> clusters, where each SiO<sub>4</sub> unit is linked through two corner oxygen ions to adjacent tetrahedra forming isolated three-fold rings. Na substitution on the Sr site will originate, for charge compensation, oxygen vacancies responsible for the oxide ion conductivity in the system, according to a mechanism still not completely clear at the moment, as both vacancy and interstitial-mediated mechanisms were discussed.<sup>4,5</sup> A neutron powder diffraction study on Na and K-doped samples excluded the presence of interstitial oxygen ions in both the systems and suggested that oxide ion vacancies, consistent with the nominal compositions, are present at r.t. and 400 °C for Sr<sub>0.6</sub>Na<sub>0.4</sub>SiO<sub>2.8</sub>, while a larger oxygen under-stoichiometry is expected at 800 °C.<sup>7</sup>

In this work we present a detailed study of the structural and transport properties of the Sr<sub>1-x</sub>Na<sub>x</sub>SiO<sub>3-0.5x</sub> series ( $x = 0.05, 0.25, 0.45$ ). We propose that the complexity of the SiO<sub>2</sub>-Na<sub>2</sub>O-SrO phase diagram must be taken into consideration, as the actual solubility degree of Na in the SrSiO<sub>3</sub> phase may be significantly lower than expected due to the possibility of formation of secondary, spurious and metastable glassy phases. We show that such secondary phases may be at the origin of the promising transport properties for this class of materials, therefore suggesting the possibility that the high conductivity values previously reported were not significantly due to oxide ion migration in the crystalline system.

Powder samples of nominal composition Sr<sub>1-x</sub>Na<sub>x</sub>SiO<sub>3-0.5x</sub> ( $x = 0.05, 0.25, 0.45$ ) were prepared by the solid state reaction according to the procedure described by P. Singh *et al.*, at a maximum synthesis temperature of 1050 °C.<sup>7</sup> Samples were slowly cooled down to room temperature (1 °C min<sup>-1</sup>). These samples will be named Na<sub>0.05</sub>, Na<sub>0.25</sub> and Na<sub>0.45</sub>, respectively. One sample of nominal composition Sr<sub>0.55</sub>Na<sub>0.45</sub>SiO<sub>2.775</sub> was subsequently retreated at 650 °C for 12 hours and slowly cooled down to room temperature (named Na<sub>0.45</sub>-RC in the following).

Department of Chemistry and INSTM, University of Pavia, Viale Taramelli 16, 27100 Pavia, Italy. E-mail: cristina.tealdi@unipv.it

† Electronic supplementary information (ESI) available: Rietveld refined NPD patterns and structural parameters; DCS measurement; XRPD of Na<sub>2</sub>Si<sub>2</sub>O<sub>5</sub>. See DOI: 10.1039/c4cc07025a



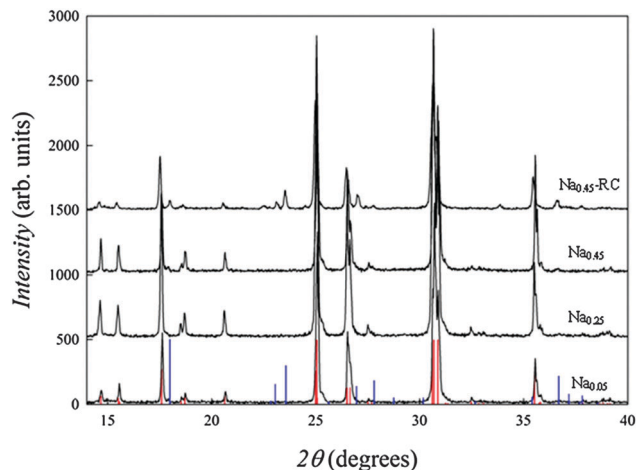


Fig. 1 XRD patterns of the  $\text{Sr}_{1-x}\text{Na}_x\text{SiO}_{3-0.5x}$  series. Vertical red lines refer to the theoretical Bragg peaks for  $\text{SrSiO}_3$ ; vertical blue lines refer to the theoretical Bragg peaks for  $\alpha\text{-Na}_2\text{Si}_2\text{O}_5$ .

Room temperature X-ray powder diffraction (XRPD) patterns of all the prepared samples were acquired on a Bruker D8-Advance diffractometer with Cu  $K\alpha$  radiation in the  $2\theta$  range 10–100 degrees, with fixed steps of 0.02 degrees and counting time per steps of 10 s. Fig. 1 shows the XRPD patterns of the  $\text{Sr}_{1-x}\text{Na}_x\text{SiO}_{3-0.5x}$  ( $x = 0.05, 0.25, 0.45$ ) series prepared at 1050 °C. All the patterns can be indexed in the monoclinic  $C12/c1$  space group (no. 15). No spurious reflections can be identified for  $\text{Na}_{0.05}$ ,  $\text{Na}_{0.25}$  and  $\text{Na}_{0.45}$ , and the patterns are consistent with the structure of the parent  $\text{SrSiO}_3$  compound.<sup>8</sup> Sample  $\text{Na}_{0.45}\text{-RC}$  clearly presents additional peaks, mainly compatible with the  $\alpha$  polymorph of  $\text{Na}_2\text{Si}_2\text{O}_5$  (see below).

Rietveld refinement<sup>9</sup> was performed using the FullProf software.<sup>10</sup> Table 1 shows the Rietveld refined cell parameters and unit cell volume obtained from the XRPD measurements for the  $\text{Sr}_{1-x}\text{Na}_x\text{SiO}_{3-0.5x}$  series prepared at 1050 °C. No clear trend is observed for the evolution of the unit cell volume along with doping. This result suggests that the substitution of Na ions for Sr might not be complete and the actual stoichiometry of the crystalline phase could therefore be different from the nominal one.

In order to assess this aspect, room temperature neutron powder diffraction (NPD) measurements were acquired on the HRPT instrument at the Paul Scherrer Institute (PSI, Villigen) in the  $2\theta$  range 10–100 degrees. Rietveld refinement allowed in this case to extract the occupancies of Na ions on the Sr site, as well as to estimate the degree of possible oxygen under-stoichiometry. Fig. 2 shows the Rietveld refined pattern for the sample of nominal composition  $\text{Sr}_{0.75}\text{Na}_{0.25}\text{SiO}_{2.875}$ . Rietveld refinements and the structural parameters for all the samples are reported as Fig. S1 and Table S1, respectively (ESI<sup>†</sup>). Analysis of the refined parameters

Table 1 X-ray, Rietveld refined lattice cell parameters and unit volume for the  $\text{Sr}_{1-x}\text{Na}_x\text{SiO}_{3-0.5x}$  series

$x$	$a$ (Å)	$b$ (Å)	$c$ (Å)	$\beta$ (°)	$V$ (Å <sup>3</sup> )
0.05	12.3530(4)	7.1558(2)	10.9009(3)	111.617(1)	895.82(5)
0.25	12.3418(3)	7.1513(2)	10.8914(2)	111.581(2)	893.89(4)
0.45	12.3536(6)	7.1527(3)	10.9046(5)	111.710(3)	895.21(8)

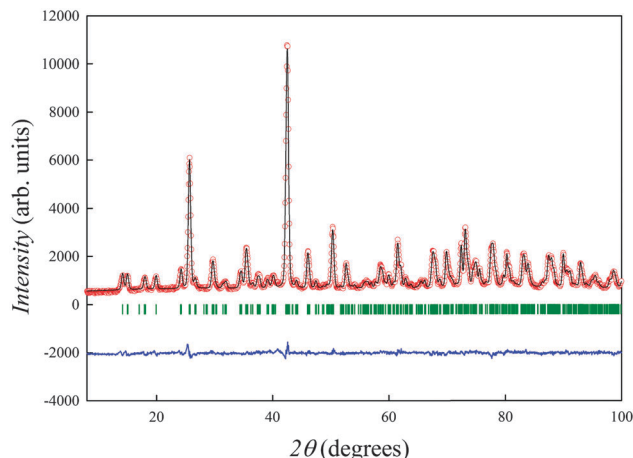


Fig. 2 Rietveld refined NPD patterns of  $\text{Sr}_{0.75}\text{Na}_{0.25}\text{SiO}_{2.875}$  showing the experimental (red circle), calculated (black line) and difference profile (blue line). Vertical green lines refer to the theoretical Bragg peaks for  $\text{SrSiO}_3$ .

(Table S1, ESI<sup>†</sup>) confirms that this series does not obey the Vegard's law for solid solutions. If allowed to change in the refinement, the Na occupancy on the Sr sites tends to zero (and the Sr site keeps the full occupancy), while the oxygen sites tend to full occupancy, so that the composition derived from the analysis of the neutron diffraction data is in agreement, within the experimental errors, with nominal  $\text{SrSiO}_3$  composition for all the three samples.

Differential Scanning Calorimetry (DSC) measurements were performed from room temperature up to 600 °C with a scan rate of 20 °C  $\text{min}^{-1}$  in  $\text{N}_2$  flux on the  $\text{Na}_{0.45}$  sample, and showed a sigmoidal feature suggestive of a glass transition just below 500 °C (Fig. S2, ESI<sup>†</sup>). Following such an indication, the sample  $\text{Na}_{0.45}$  was subsequently retreated at 650 °C for 12 hours and slowly cooled down to room temperature (sample  $\text{Na}_{0.45}\text{-RC}$ ). The XRD pattern of this sample in Fig. 1 clearly shows the appearance of additional peaks compared to those ascribed to the crystalline  $\text{SrSiO}_3$  phase. The most intense peaks among such reflections can be attributed to  $\alpha\text{-Na}_2\text{Si}_2\text{O}_5$ . Fig. S3 (ESI<sup>†</sup>) shows the two-phase Rietveld refined NPD pattern of this sample considering  $\text{SrSiO}_3$  and  $\alpha\text{-Na}_2\text{Si}_2\text{O}_5$ . A good agreement between the calculated and the experimental pattern is found by considering these two phases, with minor contributions possibly related to different  $\text{Na}_2\text{Si}_2\text{O}_5$  polymorphs or other secondary phases still unexplained.

Solid-state MAS NMR measurements were acquired on a 9.4 T magnet using a 7.0 mm probe. <sup>29</sup>Si spectra were recorded at a spinning rate of 5 kHz, at ambient temperature with a single pulse experiment (3.00  $\mu\text{s}$  pulse), a delay of 300 seconds and 4k scans. The spectra were referred to TMS.

In Fig. 3 the <sup>29</sup>Si spectra of samples  $\text{Na}_{0.05}$  (d),  $\text{Na}_{0.25}$  (c) and  $\text{Na}_{0.45}$  (b) are shown, together with the <sup>29</sup>Si spectra of the samples  $\text{Na}_{0.45}\text{-RC}$  (a) and of a properly prepared  $\text{Na}_2\text{Si}_2\text{O}_5$  glassy sample (e). The spectrum of the  $\text{Na}_{0.05}$  sample presents a single sharp peak centered at  $-86$  ppm. With the introduction of higher Na content in the structure, a new broad peak centered at  $\sim -89$  ppm appears; the relative intensity of the broad peak with respect to that of the signal at  $-86$  ppm grows along with the increase of the Na content. Fig. 3a reports the spectrum of the sample  $\text{Sr}_{0.55}\text{Na}_{0.45}\text{SiO}_3$



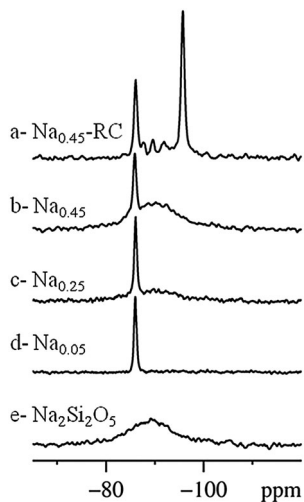


Fig. 3  $^{29}\text{Si}$  NMR spectra of samples of the  $\text{Sr}_{1-x}\text{Na}_x\text{SiO}_{3-0.5x}$  series prepared at  $1050\text{ }^\circ\text{C}$  (panel b–d),  $\text{Na}_{0.45}\text{-RC}$  recrystallized at  $650\text{ }^\circ\text{C}$  (a), glassy  $\text{Na}_2\text{Si}_2\text{O}_5$  (e). The intensities of the spectra are normalized with respect to the sharp peak at  $-86\text{ ppm}$ .

recrystallized at  $650\text{ }^\circ\text{C}$  ( $\text{Na}_{0.45}\text{-RC}$ ). For this sample, the broad signal disappears while a new sharp resonance at  $-95.7\text{ ppm}$  is observed. Other weak signals appear at  $-87.7$ ,  $-89.6$  and  $-91.9\text{ ppm}$ . We recall that for this sample, recrystallized at  $650\text{ }^\circ\text{C}$ , also the XRD data show additional peaks (Fig. 1) compared to the starting sample  $\text{Na}_{0.45}$ .

The peak at  $-86\text{ ppm}$  observed in each sample is related to the crystalline  $\text{SrSiO}_3$ -based phase.<sup>11,12</sup> The position and the broadening of this signal do not seem to be affected by the nominal composition of the samples, suggesting the formation of pure  $\text{SrSiO}_3$ , independently of the increasing amount of Na present in the starting reagent mixture. The solubility of Na in the  $\text{SrSiO}_3$  phase thus seems to be extremely low, in agreement with the NPD analysis. This hypothesis is also supported by the appearance of the broad peak at  $\sim -89\text{ ppm}$  with the introduction of Na in the system, indicative of the formation of a new disordered phase (see below and Fig. 3e) whose content increases as the nominal Na content in the sample does. This second phase has been identified with glassy  $\text{Na}_2\text{O}\cdot 2\text{SiO}_2$ . In fact, it can be formed with respect to the nominal stoichiometry of the initial mixtures for the different compositions, if we assume limited solubility of Na on the Sr site of  $\text{SrSiO}_3$ . This is confirmed by the spectrum of  $\text{Na}_{0.45}\text{-RC}$  (Fig. 3a). The peak at  $-95.7\text{ ppm}$  has been attributed to silicon in the crystalline  $\alpha\text{-Na}_2\text{Si}_2\text{O}_5$  phase.<sup>13</sup> The small peaks between  $-87$  and  $-92\text{ ppm}$  can be attributed to minor contributions from other unidentified recrystallized species, as also observed in the XRD patterns.

In order to support the identification of the glassy phase, a sample of nominal composition  $\text{Na}_2\text{Si}_2\text{O}_5$  was prepared from the solid state reaction under the same synthetic conditions used for the  $\text{Sr}_{1-x}\text{Na}_x\text{SiO}_{3-0.5x}$  series. Its NMR spectrum (Fig. 3e) clearly resembles the broad peak of the Na-containing samples. The broadening of the signal clearly evidences the amorphous nature of this product, as also confirmed by the XRD pattern (see Fig. S4, ESI†).

In order to investigate the effects of the glassy phase on the transport properties, impedance spectroscopy measurements

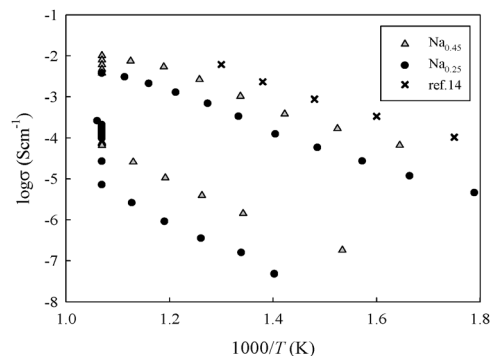


Fig. 4 Arrhenius plot of the  $\text{Na}_{0.45}$  and  $\text{Na}_{0.25}$  sample indicating the drop in conductivity during the isothermal treatment. Comparison with data derived from Na diffusion coefficient values in glassy- $\text{Na}_2\text{Si}_2\text{O}_5$  reported in ref. 14.

were performed. The powders were isostatically pressed to form  $1\text{ cm}$  diameter thin cylindrical pellets and then sintered at  $1000\text{ }^\circ\text{C}$  as described elsewhere.<sup>5</sup> Platinum-sputtered electrodes were placed on both sides of each sintered pellet. Two-probes AC impedance spectroscopy measurements were carried out under static air in the temperature range  $300\text{--}680\text{ }^\circ\text{C}$ , using a Solartron 1286 equipped with a Frequency Response Analyzer 1287 in the frequency range  $1\text{ Hz--}10\text{ MHz}$ . Isothermal acquisitions as a function of time were performed at approximately  $650\text{ }^\circ\text{C}$  in order to follow the evolution of the conductivity during the possible recrystallization of the sample. Fig. 4 shows the Arrhenius plots of conductivity for the  $\text{Na}_{0.25}$  and  $\text{Na}_{0.45}$  samples, together with data of glassy- $\text{Na}_2\text{Si}_2\text{O}_5$ .<sup>14</sup> This graph shows that a considerable drop in conductivity is achieved when the sample is maintained at a specific temperature for a certain time (overnight). The drop in conductivity is associated with the partial recrystallization of the sample, as followed *ex situ* with both XRD and NMR.

The similarity in the slope of the Arrhenius plot for glassy  $\text{Na}_2\text{Si}_2\text{O}_5$  and our samples before recrystallization is remarkable. The absolute values of conductivity of the pure glassy phase are higher than our data for the sample of nominal composition  $\text{Sr}_{0.55}\text{Na}_{0.45}\text{-SiO}_{2.775}$ . This is likely due to a dilution effect, since our samples are two-phases in nature (glassy  $\text{Na}_2\text{Si}_2\text{O}_5$  dispersed in the insulating  $\text{SrSiO}_3$  crystalline phase). The conductivity data reported in Fig. 4 are lower than those reported for the same nominal compositions<sup>5</sup> but in agreement with the data reported for  $\text{Sr}_{0.8}\text{K}_{0.2}\text{Si}_{0.5}\text{Ge}_{0.5}\text{O}_{2.9}$ .<sup>15</sup>

This study reported a powerful combination of X-ray and neutron diffraction, solid-state  $^{29}\text{Si}$  NMR, differential scanning calorimetry and impedance spectroscopy measurements used to investigate the structural and transport properties of the  $\text{Sr}_{1-x}\text{Na}_x\text{SiO}_{3-0.5x}$  series, recently indicated as a novel family of oxide ion conductors with potential high impact for SOFCs.

The results presented here clearly evidenced that the actual solubility degree of Na in the  $\text{SrSiO}_3$  phase is significantly lower than expected due to the formation of a secondary and metastable glassy phase, thus leading to a very low amount of oxygen vacancies with respect to the nominal stoichiometry. We showed that such a secondary phase may be at the origin of the promising transport properties of these materials. Most probably, the high conductivity values previously reported are due only to a limited



extent to oxide ion migration in the crystalline system, in addition to transport of Na ions in the glassy phase, in agreement with a very recent work.<sup>16</sup> This suggestion could also be consistent with the very low activation energy reported for this family of oxides compared to conventional oxide ion conductors.<sup>6</sup> We recognize that the degree of crystallization–amorphization of the system may be strongly dependent on the synthesis conditions and therefore different results, especially for what concern the conductivity data, may be obtained. However, this study suggests that attention should be paid in the interpretation of data related to compositions that may easily give origin to glassy phases, such as alkaline-doped silicates, as suggested also in our previous work.<sup>17</sup>

We are grateful to CARIPLO Foundation (project 2009-2623) and to Dr Vladimir Pomjakushin for the NPD measurements.

## Notes and references

- 1 L. Malavasi, C. A. J. Fisher and S. M. Islam, *Chem. Soc. Rev.*, 2010, **39**, 4370.
- 2 M. Li, M. J. Pietrovski, R. A. De Souza, H. Zhang, I. M. Reaney, S. N. Cool, J. A. Kilner and D. C. Sinclair, *Nat. Mater.*, 2014, **13**, 31.
- 3 C. Li, R. D. Bayliss and S. J. Skinner, *Solid State Ionics*, 2014, **262**, 530.
- 4 P. Singh and J. B. Goodenough, *Energy Environ. Sci.*, 2012, **5**, 9626.
- 5 P. Singh and J. B. Goodenough, *J. Am. Chem. Soc.*, 2013, **135**, 10149.
- 6 T. Wei, P. Singh, Y. Gong, J. B. Goodenough, Y. Huang and K. Huang, *Energy Environ. Sci.*, 2014, **7**, 1680.
- 7 R. Martinez-Coronado, P. Singh, J. Alonso-Alonso and J. B. Goodenough, *J. Mater. Chem. A*, 2014, **2**, 4355.
- 8 F. Nishi, *Acta Crystallogr., Sect. C: Cryst. Struct. Commun.*, 1997, **53**, 534.
- 9 H. M. Rietveld, *J. Appl. Crystallogr.*, 1969, **2**, 65.
- 10 J. Rodriguez-Carvajal, *Physica B*, 1993, **192**, 55.
- 11 K. A. Smith, R. J. Kirpatrick, E. Oldfield and D. M. Henderson, *Am. Mineral.*, 1983, **68**, 1206.
- 12 J. Xu, X. Wang, H. Fu, C. M. Brown, X. Jing, F. Liao, F. Lu, X. Li, X. Kuang and M. Wu, *Inorg. Chem.*, 2014, **53**, 6962.
- 13 L. Marte, S. Cadars, E. Véron, D. Massiot and M. Deschamps, *Solid State Nucl. Magn. Reson.*, 2012, **45–46**, 1.
- 14 C. Kaps, *J. Non-Cryst. Solids*, 1984, **65**, 189.
- 15 R. D. Bayliss, S. N. Cook, S. Fearn, J. A. Kilner, C. Graves and S. Skinner, *Energy Environ. Sci.*, 2014, **7**, 2999.
- 16 I. R. Evans, J. S. O. Evans, H. G. Davies, A. R. Haworth and M. L. Tate, *Chem. Mater.*, 2014, **26**, 5187.
- 17 C. Tealdi, G. Chiodelli, S. Pin, L. Malavasi and G. Flor, *J. Mater. Chem. A*, 2014, **2**, 907.

